

Articles

Discovery of Novel Hydroxamates as Highly Potent Tumor Necrosis Factor- α Converting Enzyme Inhibitors: Part I—Discovery of Two Binding Modes[†]Zhaoning Zhu,^{*,‡} Robert Mazzola,[‡] Lisa Sinning,[‡] Brian McKittrick,[‡] Xiaoda Niu,[§] Daniel Lundell,[§] Jing Sun,[§] Peter Orth,[‡] Zhuyan Guo,[‡] Vincent Madison,[‡] Richard Ingram,[‡] and Brian M. Beyer[‡]

Departments of Medicinal Chemistry and Inflammation and Infectious Diseases, Schering-Plough Research Institute, 2015 Galloping Hill Road, Kenilworth, New Jersey 07033

Received March 29, 2007

Through a de novo design approach, hydroxamates derived from *trans*-cyclopropyl dicarboxylate were examined as potential TNF- α converting enzyme (TACE) inhibitors. Two distinctive series of inhibitors (A and B) were identified and shown to have different structure–activity relationship trends and selectivity profiles against other matrix metalloproteases despite their close structural similarities. X-ray crystallography of the inhibitors binding to the TACE enzyme demonstrates that each series derives its activity from the opposite enantiomer of the cyclopropyl scaffolds, which display almost superimposable hydroxamate groups that coordinate to the zinc at the catalytic site. Mode A inhibitors occupy the S1'–S3' binding pockets, whereas mode B resides in the nonprime binding sites.

Introduction

Overexpression of tumor necrosis factor α (TNF- α), a 17 kDa pro-inflammatory cytokine, has been directly associated with inflammation diseases such as rheumatoid arthritis and Crohn's disease.¹ Reduction of TNF- α levels through a scavenging mechanism using either antibodies or TNF- α receptor fusion proteins has been highly effective in controlling the symptoms of these diseases in various clinical trials.² TNF- α is released from the membrane-bound pro-TNF- α —a 26 kDa precursor protein³—through a proteolytic cleavage process mainly involving the TNF- α converting enzyme or TACE (ADAM17), which is a member of the zinc-metalloprotease family known as ADAM (a disintegrin and a metalloprotease).⁴ Inhibition of TACE activity to control the level of TNF- α release has long been viewed as a promising way of treating related inflammatory diseases.⁵

Many known small molecule TACE inhibitors are related to the first generation succinate-based hydroxamate peptidic matrix metalloprotease (MMP) inhibitors.⁶ Most of these contain three important structural motifs: a zinc binding element—commonly a hydroxamate; a hydrogen bond acceptor—usually an amide or sulfonamide—placed 3–4 bonds away; and a hydrophobic group attached on the backbone (**2**, Figure 1). The backbones of these inhibitors are usually rigidified through cyclization, which might enhance the binding affinity and selectivity and improve their pharmacokinetic profiles. The selectivity of TACE inhibitors against other MMPs and ADAMs has been considered to be important for drug development but difficult to achieve. For example, ADAM10 has the highest aminoacid sequence homology as compared with TACE among all known MMPs. ADAM10 also cleaves the membrane-bound TNF- α precursor

protein to its mature soluble form in vitro. It is also involved in the processing of several cell–surface proteins including Hb-EGF,⁷ ephrin-A2,⁸ APP,⁹ and Notch.¹⁰ ADAM10 deficiency in mice is lethal at the embryonic stage. Despite the fact that a few TACE inhibitors have advanced to human clinic trial stages, one of which was **3** (DPC-333, Figure 1),¹¹ so far, no TACE inhibitor drug has reached the market. This has been partially attributed to the general lack of selectivity for these early hydroxamate TACE inhibitors. Thus, identification of a highly selective TACE inhibitor has been a major goal for many academic and pharmaceutical industry research laboratories.

Docking studies of **3** with the published TACE X-ray crystal structure¹² suggested that the hydroxamate coordinates to the zinc atom in a bidentate fashion with the lactam carbonyl group interacting with the hydrogen bond donors of Leu-348 and Gly-349 in TACE.¹³ The hydrophobic group extends into the S1'–S3' binding pockets. In our effort to search for novel TACE inhibitors, we examined the possibility of arranging the three binding elements in a general structure **1** where a hydroxamate derived from the *trans*-cyclopropyl dicarboxylate would offer a good opportunity to interact with the zinc metal and the second carbonyl group would be in a position to pickup the H-bonding interactions with Leu-348 and Gly-349. A hydrophobic group could be attached to the cyclopropyl ring to reach into the prime site binding pockets even though the available protein crystal structure, which was obtained with a peptidic hydroxamate inhibitor without a S3' group, did not seem to tolerate the hydrophobic group in compound **3** without significant protein rearrangement. Realizing that the only TACE protein crystal structure available to us at the time would not help us rank order different designs of the hydrophobic group, we decided to prepare all four scaffolds (**4–7**) in Figure 2 to examine their potential TACE inhibitory activities. These four scaffolds differ by the spacers through which the benzyl group is attached to the cyclopropyl ring as well as the substitution pattern on the

[†] Dedicated to Professor Howard E. Zimmerman on his 82nd birthday.

* To whom correspondence should be addressed. Tel: 908-740-5651. E-mail: Zhaoning.Zhu@spcorp.com.

[‡] Department of Medicinal Chemistry.[§] Department of Inflammation and Infectious Diseases.

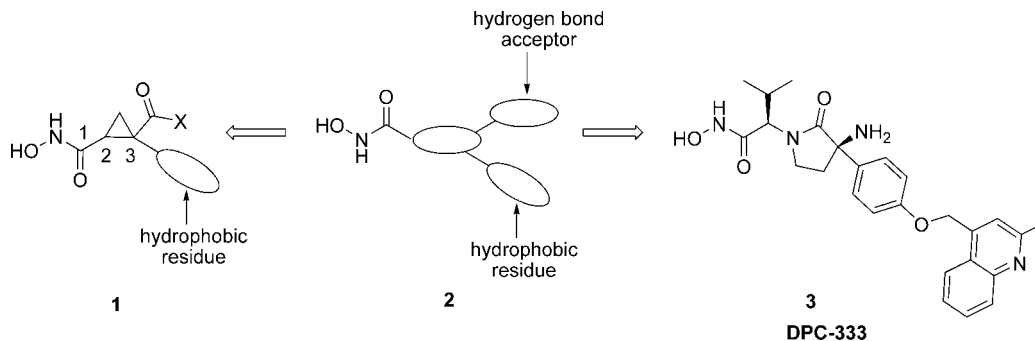


Figure 1. TACE inhibitor pharmacophore model.

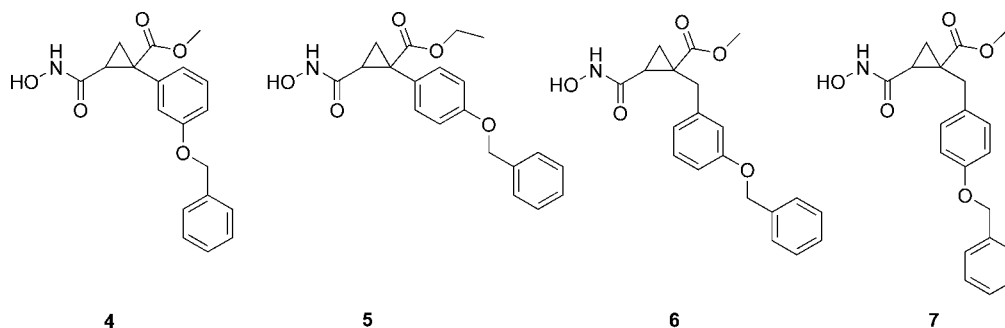
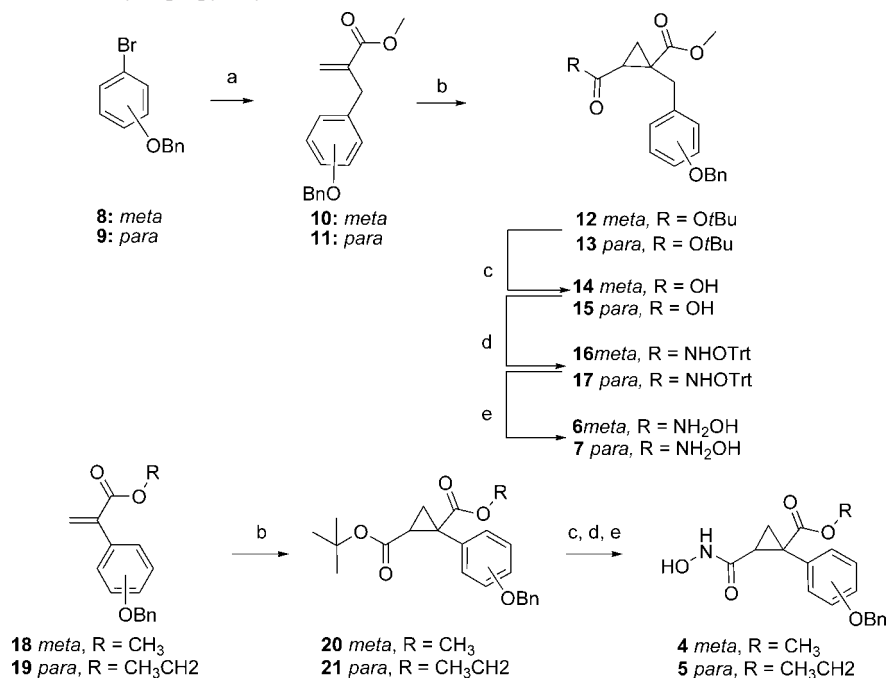


Figure 2. Scaffold design.

Scheme 1. Synthetic Scheme for Cyclopropyl Hydroxamates^a



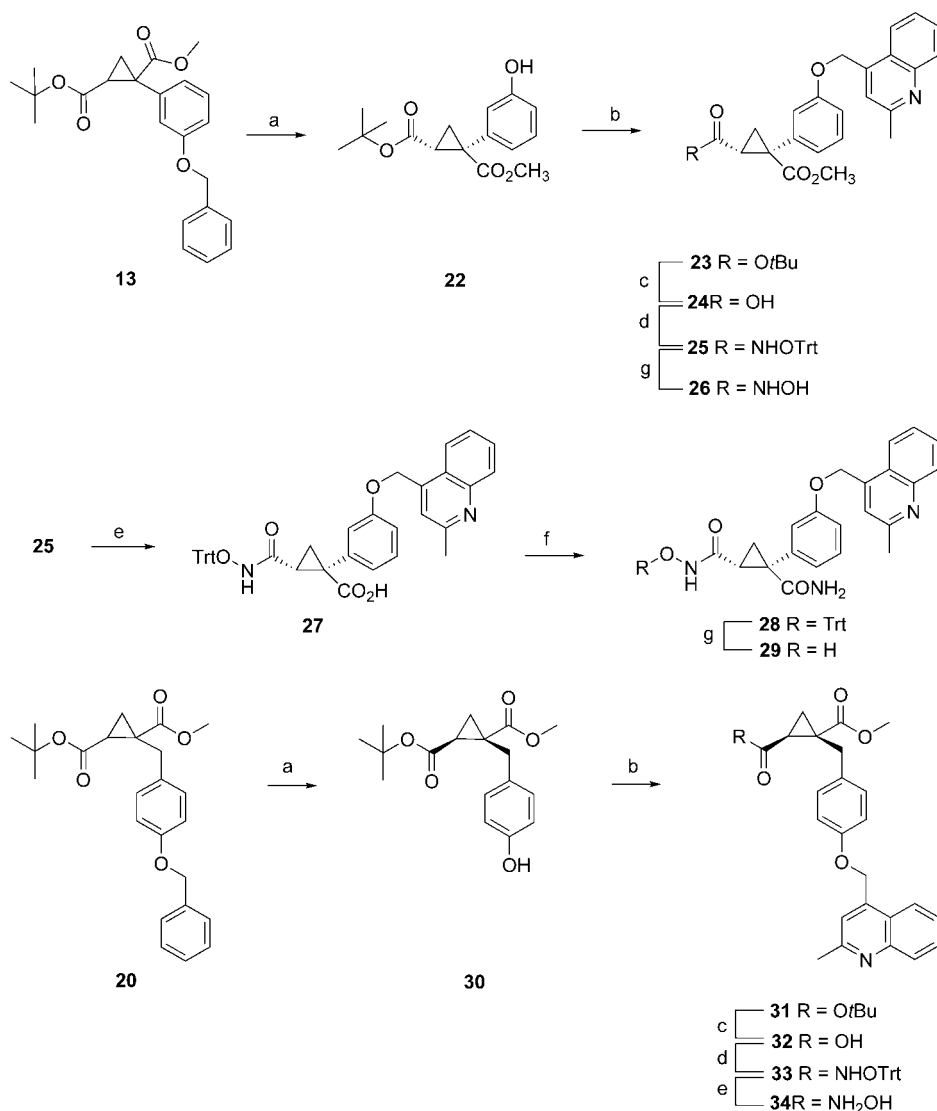
^a Reagents: (a) (1) *n*-BuLi, -78°C , 1 h; (2) CuCN, 0°C , 30 min; (3) methyl 2-(bromomethyl)acrylate, THF, -78°C , 30 min; (4) -78 to -10°C . (b) DBU, *t*-butyloxymethyl-tetrahydro-thiophenium bromide, CH₃CN. (c) 30% TFA, CH₂Cl₂. (d) *O*-Tritylhydroxyl amine, HOBt, EDCI, NMM, CH₂Cl₂. (e) (CH₃CH₂)₃SiH, 30% TFA, CH₂Cl₂.

phenyl or benzyl group, which would offer slightly different geometries to orient the hydrophobic group for optimal binding in S3'.

Chemistry

These four cyclopropyl scaffolds were obtained via a cyclopropanation reaction involving appropriate precursor acrylates

and 1-*tert*-butoxycarbonylmethyl-tetrahydrothiophenium bromide (Scheme 1). Cuprates generated from *meta/para*-benzyloxyphenyl bromides **8/9** reacted with methyl α -bromomethylacrylate to give the *meta/para*-benzyloxybenzylacrylates **10/11**, respectively.¹⁴ Acrylates **18** and **19** were obtained using a literature procedure.¹⁵ All four acrylates (**10**, **11**, **18**, and **19**) readily gave the desired *trans*-dicarboxylate cyclopropanation

Scheme 2. Chiral Resolution of Intermediate and Solution Phase Chemistry for SAR Development^a

^a Reagents: (a) (1) H₂, 10% Pd/C, CH₃OH; (2) OD Chiral Column, 5% IPA/hexane. (b) 4-Chloromethyl-2-methylquinoline, K₂CO₃, TBAB, CH₂Cl₂. (c) 30% TFA, CH₂Cl₂. (d) *O*-Tritylhydroxyl amine, HOAt, EDCI, DIPEA, CH₂Cl₂. (e) LiOH, 1:1 THF:H₂O. (f) NH₄Cl, HOBT, EDCI, DIPEA, DMF. (g) (CH₃CH₂)₃SiH, 30% TFA, CH₂Cl₂.

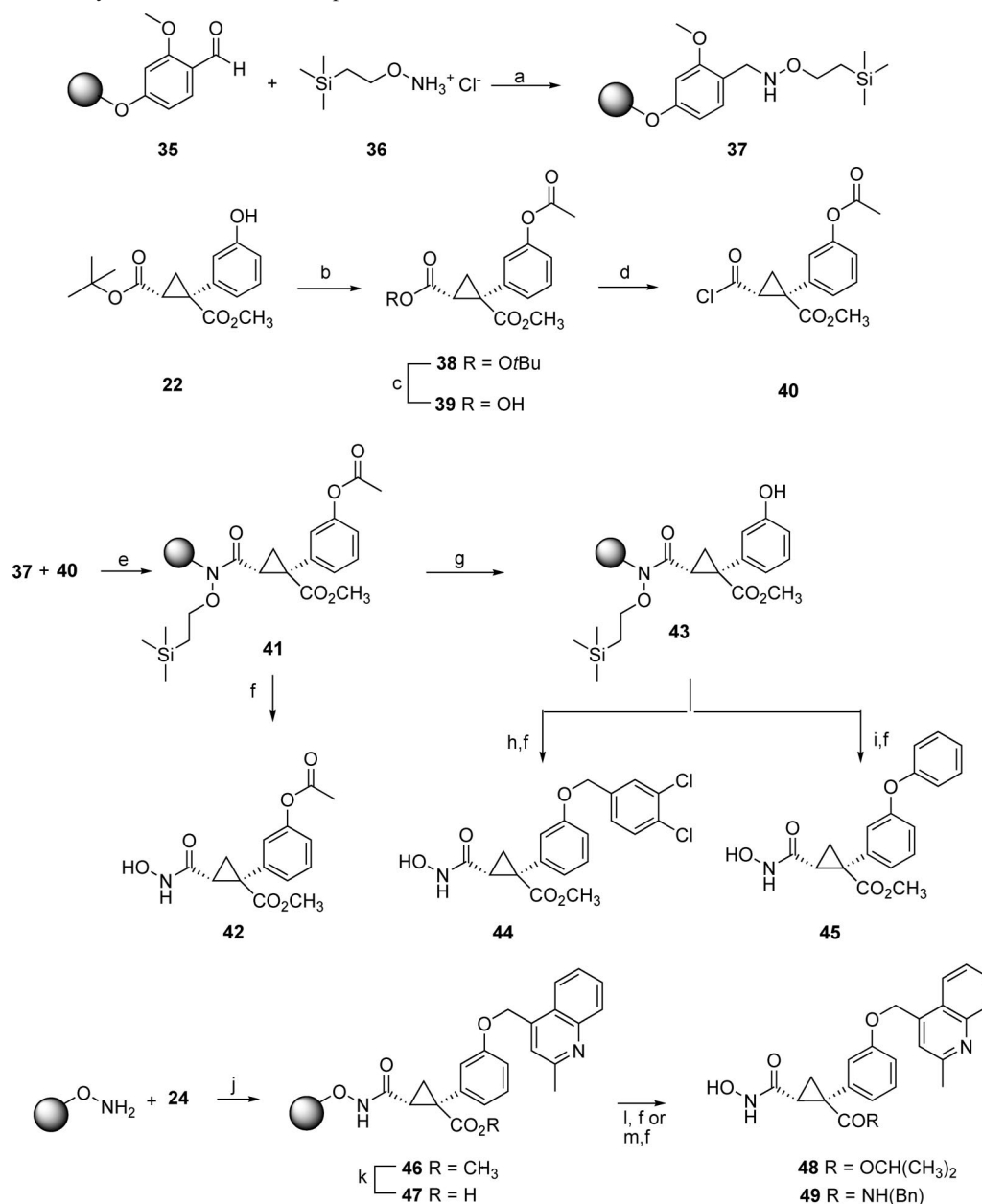
products (**12**, **13**, **20**, and **21**) with exclusive *trans*-selectivity.¹⁶ After removal of the *tert*-butyl esters, the resulting acids were coupled with *O*-trityl hydroxylamine using a standard peptide coupling condition followed by deprotection of the trityl group to give **6**, **7**, **4**, and **5**, which were found to have TACE *K*_i values of 4, 0.8, 0.5, and 20 μ M as racemic mixtures, respectively.

We concentrated our effort on two scaffolds, **4** and **7**, for subsequent follow-up, primarily focused on two sites for SAR developments: (i) replacement of the benzyl group and (ii) ester modifications. At first, the benzyl groups in core intermediates **13** and **20** were removed through hydrogenation and the corresponding racemic phenols were resolved using an OD chiral column eluting with 5% isopropanol in hexane (Scheme 2). It was subsequently found that the TACE binding affinity was exclusively associated with the enantiomer that eluted second for the phenylcyclopropyl series (**22**) and the enantiomer that eluted first for the benzylcyclopropyl series (**30**). Alkylation of the appropriate enantiomer of **22** led to compound **23** followed by deprotection of the *tert*-butyl ester to give an acid. The resulting acid was coupled with *O*-trityl hydroxylamine to give protected hydroxamate **25**. Subsequently, compound **25** was converted to **26** through deprotection of the trityl group.

Additionally, hydrolysis of **25** followed by amide formation and hydroxamate deprotection led to **29**. Similarly, compound **20** was converted to **34** using the same procedure.

To rapidly explore phenol SAR, a solid-phase synthesis for ethers from a resin-bound phenol was developed.¹⁷ This required a resin linker for the hydroxamate that would not leave an alkylatable site, such as -OH or -NH-, on the linked hydroxamate group to carry out the subsequent solid-phase *O*-alkylation or *O*-arylation on the phenol.¹⁸ It seemed that an *N*-linked *O*-trimethylsilylethylhydroxamine (**37**) would offer a good opportunity to achieve this. Thus, *O*-trimethylsilylethylhydroxamine was loaded onto aldehyde resin **35** through oxime reduction using either borane-pyridine or cyanoborohydride under acidic conditions. The resin-bound hydroxylamine was acylated with acid chloride **40**, generated from chiral intermediate **22**, and the loading level was found to be 0.40 mmol/g, determined after cleavage to afford compound **42**.

After removal of the acetyl group from the resin bound **41** with 20% piperidine in DMF, the resulting resin-bound phenol **43** was alkylated or arylated¹⁹ using either alcohols through Mitsunobu condition or aryl boronic acid through copper acetate-mediated *O*-arylation chemistry to give **44** or **45**, respectively,

Scheme 3. Solid Phase Synthesis for SAR Development on Phenols^a

^a Reagents: (a) (1) 10:20:70 CH₃CO₂H:CH₃OH:THF; (2) BH₃-pyridine, CH₂Cl₂. (b) Acetic anhydride, DMAP, CH₂Cl₂. (c) 30% TFA in DCM. (d) Oxalyl chloride, CH₂Cl₂ with 1 drop of DMF. (e) DIPEA, DCM. (f) 50% TFA, CH₂Cl₂. (g) 20% piperidine in DMF. (h) ADDP, 3,4-dichlorobenzyl alcohol, PBu₃, THF. (i) Cu(OAc)₂, DIPEA, phenyl boronic acid, DCM. (j) EDCI, NMM, HOAt, CH₂Cl₂. (k) 1 M Bu₄NHOH, THF, 60 °C. (l) 2-Propanol, EDCI, DMAP, CH₂Cl₂. (m) Benzyl amine, EDCI, HOBT, NMM, NMP. (a) Superimposition of X-ray crystal structures of compound **34** and **26** in the TACE enzyme (V353G). (b) Key interaction of **34** (green) with TACE enzyme (V353G). (c) Key interactions of **26** (yellow) with TACE enzyme (V353G).

after TFA cleavage/deprotection followed by HPLC purification. Similarly, compound **24** was loaded on to commercially available hydroxylamine resin. The ester group was hydrolyzed, and the resulting acid was converted to ester or amide through a routine solid-phase transformation to give **48** and **49** after TFA cleavage and purification.

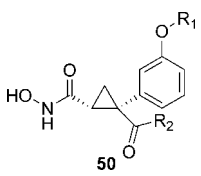
The TACE activities were measured by an internally quenched peptide substrate with its sequence derived from the pro-TNF α cleavage site using a catalytic domain of recombinant human TACE enzyme. The K_i values are listed in Table 1 for hydroxamates derived from **22**. The eudismic ratios for inhibitors derived from **22** and **30** are high with over 300-fold for compound **4** and 39-fold for compound **77**, prepared from the

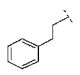
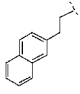
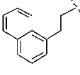
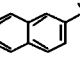
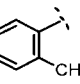
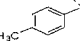

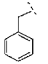
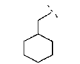
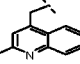
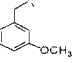
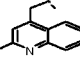
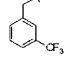
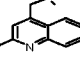
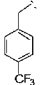
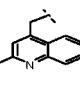
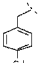
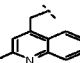
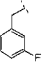
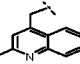
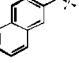
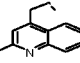
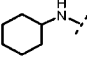
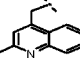
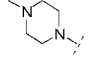
individual enantiomers of **22** and **30**, respectively (entry 1 in Table 1 and entry 2 in Table 2).²⁰

Results and Discussion

The fact that two out of the first four prototype racemic hydroxamates (Figure 2) had submicromolar TACE K_i values offered much needed proof of principle for these novel hydroxamates as potential TACE inhibitors. Because of the close structural similarities between **4** and **7**, it was speculated that the geometric requirement of the TACE S1'/S3' binding pocket can be met with either the meta-substituted phenyl or a para-substituted benzyl group directly attached to the cyclopropyl ring. However, some SAR trends differentiated these two series from the very beginning.

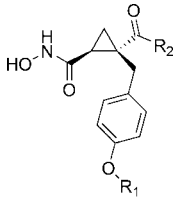
Table 1. SAR for Phenylcyclopropyl Scaffold

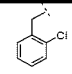
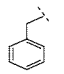
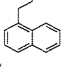
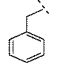
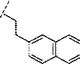
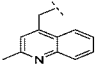
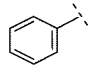
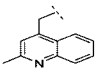
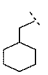
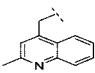

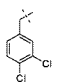



cmpnd	R1	R2	TACE Ki (nM) ^b	cmpnd	R1	R2	TACE Ki (nM) ^b
4 ^a			190	60		-OMe	290
26			12	61		-OMe	60
29			700	62		-OMe	50
44			11	63		-OMe	70
45			1100	64		-OMe	240
48			8	65		-OMe	140
49			140	66		-OMe	1600
52 ^a		-NH ₂	1200	67		-OMe	900
53	-Me	-OMe	3000	68		-OEt	16
54		-OMe	110	69		-N(H)iPr	5
55		-OMe	70	70		-N(H)Me	100
56		-OMe	18	71		-NMe ₂	2700
57		-OMe	50	72		-N(H)Ph	11
58		-OMe	80	73		-N(Me)Bn	3000
59		-OMe	3000	74			9
				75			5000

^a Racemates. ^b Each K_i value is an average of three determinations, and the standard errors for all K_i determinations are less than 10%.

Table 2. SAR for Benzylcyclopropyl Scaffold



51				51			
compnd	R1	R2	TACE Ki (nM) ^b	compnd	R1	R2	TACE Ki (nM) ^b
34			8	82		-OMe	260
76 ^a		-OMe	800	83		-OMe	>100000
77 ^a		-NH2	360	84		-OMe	>100000
78		-NH2	3	85		-OEt	3100
79		-N(H)Me	14	86		-OMe	26000
80		-NMe2	1	87		-OMe	420
81		-OMe	130	88		-NH2	80

^a Racemates. ^b Each K_i value is an average of three determinations, and the standard errors for all K_i determinations are less than 10%.

Because the carboxyl group was designed to interact with Leu-348 and Gly-349 through hydrogen-bonding interactions, an amide group should give a higher binding affinity than the corresponding ester. While the amides had comparable or lower K_i values as compared to corresponding esters for series **51** (Table 2, **76** vs **77**, **34** vs **78**, and **87** vs **88**), it was interesting to find that the carbomethoxyl group had a lower TACE K_i than the primary amide in series **50** (Table 1, **4** vs **52** and **26** vs **29**). Additionally, tertiary-amides for this scaffold (**50**) were not tolerated (Table 1, **71**, **73** and **75**), while the tertiary-amide was among the inhibitors with the highest binding affinities for series **51** (Table 2, **80**), suggesting that the carboxyl groups in scaffolds **50** and **51** did not have exactly the same interactions with the TACE enzyme.

Furthermore, the phenol substitution in the series represented by **50** tolerated a wide variety of groups such as substituted benzyls (Table 1, **44**, **52**, and **54–58**) with 3,4-dichlorobenzyl as the most potent (~ 11 nM) and (naphthyl-2-yl)methyl as the least active in this group, although still comparable with the *O*-Me ether (~ 3 μ M; Table 1, **44**, **53**, and **59**). However, the naphthylethyl ethers recovered much binding affinity (Table 1, **61** and **62**), and even the phenethyl group was comparable with the benzyl group (Table 1, **60** and **4**). Some *O*-aryl substitutions were somewhat less potent (Table 1, **45** and **63–65**), but the β -naphthyl group (**63**) retained good affinity with a TACE K_i of 72 nM. Most aliphatic groups were less tolerated (Table 1, **66** and **67**). On the other hand, the SAR on the phenol group for scaffold **51** was far more restrictive; all substituted benzyl groups were 20- to over 100-fold less potent than the (2-methylquinolin-4-yl)methyl group (Table 2, **81** and **82** vs **34**). Ethylene-tethered naphthyl groups were far less active in contrast with SAR with scaffold **50** and so were phenyl and cyclohexylmethyl groups (Table 2, **83–86**). While these divergent SAR trends for the groups initially designed to reach the

Table 3. Selectivity of TACE Inhibitors^a

compd	MMP1	MMP2	MMP3	MMP7	MMP14	BMP1	ADAM10
26	>8300	3400	1300	>8300	7700	1400	4
34	>12500	1100	100	200	1800	2200	>7000
44	6800	2800	600	5400	2400	400	10
48	7400	1400	1500	12400	3000	800	4
56	1800	>600	200	>600	4000	700	8
78	9000	300	20	40	1000	9000	12000

^a Selectivity is expressed as K_i /TACE K_i . Each K_i value is an average of three determinations, and the standard errors for all K_i determinations are less than 10%.

same S1'–S3' binding pocket could have resulted from the differences between the geometries of these two scaffolds, these differences were big enough to raise the question as to whether these classes of inhibitors did actually bind in the same pockets of the TACE enzyme.

Third, the selectivity profiles for TACE inhibitors derived from both scaffolds **50** and **51** were very different against other metalloproteases (Table 3). Most notably, inhibitors from **50** had high selectivity against MMP1, -2, -3, and -14 and BMP1 but not ADAM10 (Table 3, **26**, **44**, **48**, and **56**). On the other hand, the selectivity of inhibitors from **51** was universally high against ADAM10 while the selectivity against MMP3 and -7 varied greatly depending on the phenol-*O* substitutions (**34** and **78**). These two series of MMP/ADAM inhibitors (**50/51**) seemed to have very different presentations of pharmacophores to the class of Zn-metalloproteases, in sharp contrast to the close similarities between the chemical structures of the two scaffolds.

Lastly, under identical chiral resolution conditions, compound **22** is the second enantiomer coming out of the OD column while compound **30** is the first. Even though this alone may be circumstantial, it does raise a possibility that the two classes of TACE inhibitors are from different enantiomer series. This was subsequently confirmed with X-ray

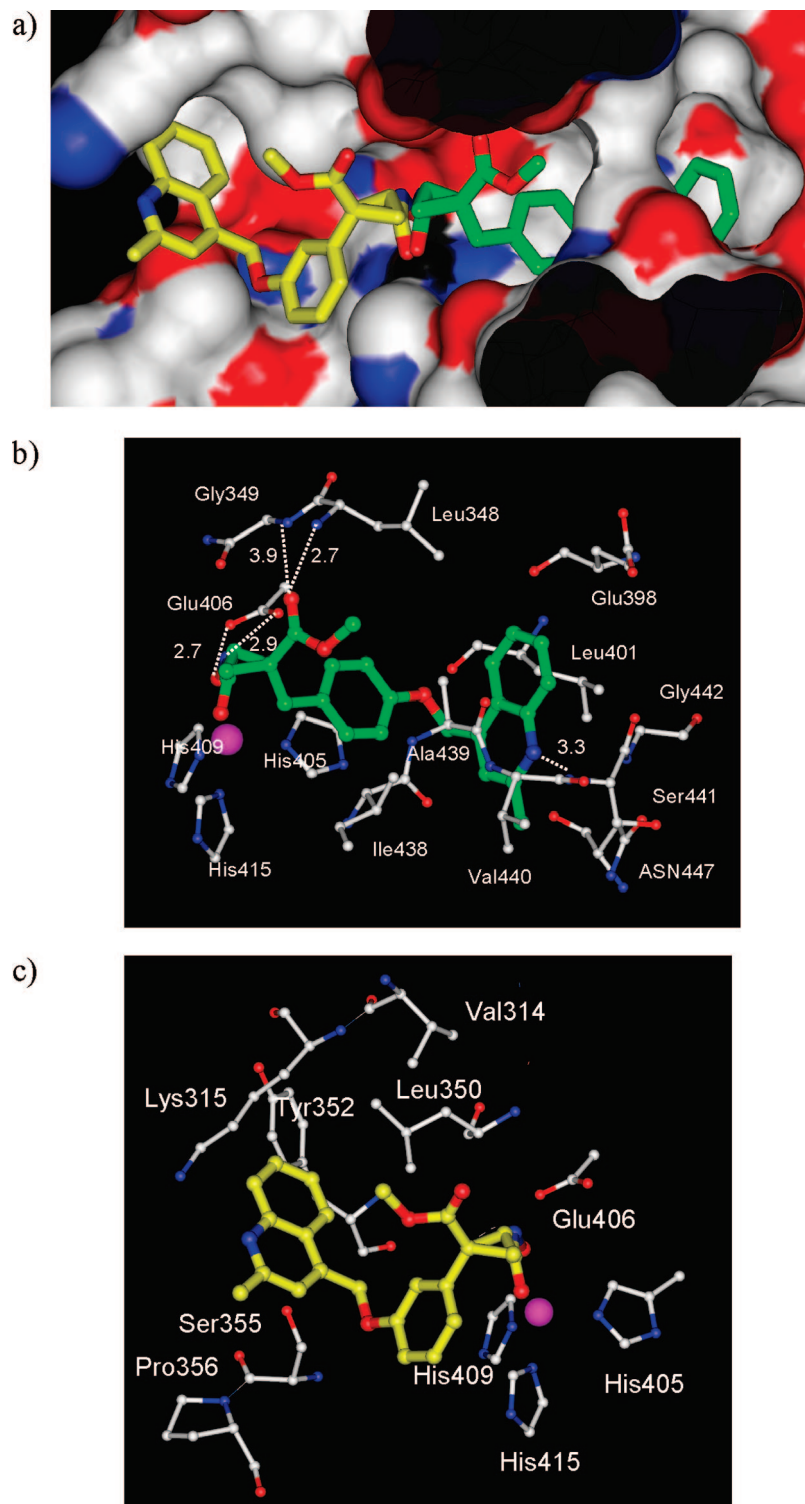


Figure 3. (a) Superimposition of X-ray crystal structures of compounds **34** and **26** in the TACE enzyme (V353G). (b) Key interaction of **34** (green) with TACE enzyme (V353G). (c) Key interactions of **26** (yellow) with TACE enzyme (V353G).

crystallography of **34** (Table 2) and **26** (Table 1) binding to a TACE mutant enzyme (V353G)²¹ with the superimposed view presented in Figure 3a. Both inhibitors used the hydroxamate group to bind to the zinc metal and formed hydrogen-bonding interactions with Glu406 with nearly identical geometry. Compound **34** had a 1*S*,2*S* configuration, and the benzyl group that attached to the cyclopropyl ring extended into the S1' binding pocket. The phenyl group formed a ring-stacking interaction with the imidazole group of the side chain of His405, and it was also packed against the hydrophobic side

chain of Ala439 and Leu348 (Figure 3b). The quinoline group occupied the extended S3' binding pocket defined by Glu398, Leu401, Ala439, Ser441, and Asn447, just as the original design. We termed this binding mode A. The mode A inhibitors bind to the enzyme, in a fashion similar to cases reported by Letavic and co-workers,²² with a conformational change of the enzyme loop region (Ala-439 to Gly-442) caused by accommodation of the quinolinyl group; for example, Val-440 shifts up 5.5 Å in comparison with the enzyme with the peptidic inhibitor. This flexible loop was

less ordered in comparison to the crystal structure of TACE with a peptidic inhibitor as reported by Maskos and co-workers⁷ due to lack of the hydrogen-bonding interactions of the peptidic inhibitor to both sides of the binding groove. The carbomethoxyl group indeed interacted with Leu-348 and Gly-349 through H-bonding interactions, which supported the SAR trend that some of the amides were among the most potent TACE inhibitors in this series. It was obvious that the S3' binding pocket was deeply buried, and it correlated well with the finding that the structural tolerance for the phenol derivatives was low. The quinoline nitrogen was within hydrogen-bonding distance with the backbone N-H of Ser441 (3.3 Å). Also, the trajectory from the S1' pocket extending to S3' fit well with a -OCH₂- linkage and that the biaryl ether or arylolethyl ethers would not appropriately place the hydrophobic terminal aryl group into the S3' binding pocket.

Compound **26**, on the other hand, extended in the opposite direction using the cyclopropyl scaffold with 1*R*,2*R* configuration, which we termed mode B. In this binding mode, the protein did not undergo significant conformational change at the S3' site. The carbomethoxyl group resided in the S1 binding pocket that was defined by side chains of Val314, Lys315, and Leu350. The pocket was half solvent-exposed and was hydrophobic in nature. As the result, hydrophobic groups such as esters were preferred at this site and over primary amides. Tertiary amides were not tolerated in this series due to the intramolecular conformational change of the phenyl induced by the tertiary-amide nitrogen. The *m*-phenyl group that attached to the cyclopropyl ring made an edge to face interaction with the imidazole group of His415 and was surrounded by the side chain of Ser355. However, because the backbone conformation of Ser355 and Pro356 in the mutant TACE enzyme was quite different in comparison with the WT due to the single residue mutation (V353G), it was not clear how much these changes had affected the binding affinity with the mutant TACE enzyme. The terminal quinolinyl group extended into the S3 binding pocket and made van der Waals contact with the hydrophobic part of the side chains of Lys315 and Tyr352. This binding pocket was also half-exposed to solvent. This explained why this site tolerated a variety of groups on the phenol oxygen, including substituted benzyl, aryl, and arylolethyl groups (Figure 3c).

The discovery of two distinctive binding modes warranted major revisions of the pharmacophore models for the design of inhibitors for TACE and other metalloproteases. In addition to the aforementioned pharmacophore model that accounted for the large majority of TACE inhibitors, which utilized the prime side binding pocket, this work further demonstrated that an alternative binding mode that placed the inhibitor into the nonprime site to obviate a hydrogen-bonding interaction with the backbone could provide potent TACE inhibitors. A search in the patent literature revealed additional examples of this type of TACE/MMP3 inhibitor.²³ It was intriguing to explore the combination of both types of binding modes for the benefit of binding affinity as well as selectivity profile against other metalloproteases. Given the structural diversity of known TACE inhibitors in the literature, it was highly possible that some of these known TACE inhibitors had already taken advantage of both prime and nonprime site binding pockets and might possess different selectivity profiles as a result.

In summary, the development of SAR for a series of de novo-designed cyclopropyl dicarboxylate-related hydroxamates led to the discovery of two series of potent TACE inhibitors. The

inhibitors bind to the TACE enzyme in two different modes as established by X-ray crystallography and exhibited different selectivity profile against other metalloproteases. Having both ADAM10 selective (mode A) and nonselective (mode B) series provided an opportunity to further evaluate the biochemical pathways and mechanism of action of these TNF- α inhibitors.

Experimental Section

Molecular Modeling. The X-ray structure of a TACE-inhibitor complex (pdb code 1BKC)⁷ was adapted for modeling before in-house crystal structures were available. One of the four molecules in the asymmetric unit was used (chain A) with a peptide inhibitor (1BKC), which showed three key features of binding: (i) zinc ligand, (ii) hydrogen bonding to the backbone NHs of Leu-348 and Gly-349, and (iii) hydrophobic interactions with residues in the S1' pocket. While the coordinates of the hydroxamate moiety were obtained from this X-ray structure as well as the X-ray structures of other nonpeptidic MMP and TACE inhibitors in various binding modes, several possible scaffolds were evaluated using docking softwares such as GLIDE (Schrodinger) and GOLD (Cambridge Crystallographic Data Center). To reduce the size of the system and therefore speed up the computation, residues that were more than 12 Å away from the original bound inhibitor were deleted. The Sybyl (Tripos) molecular modeling software package was used for molecular manipulations such as adding hydrogen atoms and assigning atomic partial charges, as well as to perform dynamics simulations and minimizations. A distance constraint of 2.0–2.2 Å from the zinc was imposed on the two hydroxamate oxygens to maintain the distance close to that observed in the crystal structures. The hydroxamate was deprotonated, and one of the carboxylate oxygens (OE1) was protonated following the finding from an early publication.²⁴

X-ray Crystallography. Prior to crystallization, TACE (V353G) was incubated with a 2-fold excess of TAPI-1 (see ref 15) and transferred into 25 mM TrisHCl at pH 8. Crystals were obtained using the hanging drop method and PEG 6000, 10% 2-propanol, and 100 mM sodium citrate, pH 5.6, as the precipitant. Crystals were soaked in the precipitant solution with the respective inhibitors for 3 days and frozen in liquid nitrogen with 15% glycerol as a cryoprotectant. Diffraction data were collected at 100 K using the IMCA-CAT beam line BM17. Data processing was performed using the HKL2000 and CCP4 packages. The crystals were orthorhombic with space group $P2_12_12_1$ and unit cell dimensions of $a = 73$, $b = 75$, and $c = 103$ Å with a resolution of 1.7 Å. There were two molecules in the asymmetric unit, and the crystal structure was determined by molecular replacement using the program AMORE²⁵ and the protein data bank entry 1BKC as a model. The structure refinement was carried out using the CNX package.^{26,27}

TACE and Metalloprotease Assays. The catalytic domain of recombinant human TNF-converting enzyme [TACEcat, residues 215–477 with two mutations (S266A and N452Q) and a 6xHis tail] was purified from the baculovirus/Hi5 cells expression system using affinity chromatography. MMPs (MMP1, -2, -3, and -7) and ecto domain of ADAM10 (a disintegrin containing metalloprotease) as well as MMP substrates 1 and 2 were purchased from R&D Systems (Minneapolis, MN). TACE, ADAM10, and MMP activities were determined by a kinetic assay measuring the rate of increase in fluorescent intensity generated by the cleavage of an internally quenched peptide substrate. The substrate for TACE was an internally quenched peptide (MCA-Pro-Leu-Ala-Gln-Ala-Val-Arg-Ser-Ser-Ser-Dpa-Arg-NH₂) [MCA, (7-methoxycoumarin-4-yl)acetyl; Dpa, *N*-3-(2,4-dinitrophenyl)-L-2,3-diaminopropionyl], with its sequence derived from the pro-TNF α cleavage site. Fifty microliters of assay mixture contained 20 mM HEPES, pH 7.3, 5 mM CaCl₂, 100 μ M ZnCl₂, 2% DMSO, 0.04% methylcellulose, 30 μ M peptide substrate, 0.1 nM TACEcat, and varying concentrations of a compound. The reaction was started by the addition of the substrate. The fluorescent intensity (excitation at 320 nm, emission at 405 nm) was measured every 45 s for 30 min using a fluorospectrometer (GEMINI XS, Molecular Devices). ADAM10 was assayed in the

same way as TACE. Substrates **1** and **2** were used in assays for MMP-1, -2, -3, and -7 according to the manufacturer's protocol. Values of K_i were calculated by the PRISM program based on one-site competitive inhibition mode. Each K_i value was an average of three determinations, and the standard errors for all K_i determinations were less than 10%.

Synthesis. All reagents were obtained from commercial sources unless noted otherwise. All NMR data were collected on 400 MHz NMR spectrometers unless otherwise indicated. The chemical shifts were expressed as ppm downfield from tetramethylsilane or as relative ppm from designated reference peaks. Preparative reverse-phase HPLC with a C-18 column using a gradient of 5–95% MeCN/water with 0.1% TFA and a mass-triggered fraction collection system was used to purify the hydroxamates. The purity of final compounds was analyzed on an ES-LCMS analytical reverse-phase HPLC system equipped with a 4.5 mm \times 100 mm, 5 μ m, C18 column and a mass detector and a UV detector monitored at both 219 and 254 nm. All runs were carried out at room temperature with a 10 min gradient of 5–95% MeCN/water with 0.1% TFA at a flow rate of 1 mL/min. See the Supporting Information for compound purity analysis data for selected compounds.

(tert)-Butyl 2-(4-Benzyloxyphenyl)-2-trans-carboethoxycyclopropane Carboxylate (21). A mixture of **19** (750 mg, 2.70 mmol), *tert*-butyloxycarbonylmethyl-tetrahydrothiophenium bromide (822 mg, 2.9 mmol), and DBU (0.61 mL, 608 mg, 4.5 mmol) in acetonitrile was stirred at room temperature for 2 days. The reaction was poured into a saturated aqueous NH_4Cl and CH_2Cl_2 mixture. The aqueous layer was extracted with CH_2Cl_2 (3 \times). The organic extracts were combined, dried over sodium sulfate, filtered, and concentrated. The crude material was chromatographed with 10–20% EtOAc/hexane to give 950 mg of **21** (68%). ^1H NMR (400 MHz, CDCl_3): δ 7.44–7.30 (m, 5H, ArH), 7.23–7.19 (m, 2H, ArH), 6.93–6.89 (m, 2H, ArH), 5.05 (s, 2H, OCH_2Ar), 4.19–4.04 (m, 2H, $\text{CO}_2\text{CH}_2\text{CH}_3$), 2.62 (dd, 1H, $J = 6.6$ Hz, 8.1 Hz, cyclopropyl-CH), 1.93 (dd, 1H, $J = 4.4$ Hz, 6.6 Hz, cyclopropyl-CH), 1.80 (dd, 1H, $J = 4.4$ Hz, 8.1 Hz, cyclopropyl-CH), 1.20–1.17 (m, 12 H, $\text{CO}_2\text{C}(\text{CH}_3)_3$, $\text{CO}_2\text{CH}_2\text{CH}_3$).

2-(4-Benzyloxyphenyl)-2-trans-carboethoxycyclopropane Hydroxyamic Acid (5). A solution of **21** in 30% trifluoroacetic acid in CH_2Cl_2 was stirred at room temperature. After 4 h, the reaction mixture was concentrated. The residue was adjusted to pH \sim 9.5 with a 1:1 ratio of a saturated NaHCO_3 : Na_2CO_3 solution. The aqueous solution was washed with ether (3 \times). After acidification to pH \sim 2, the aqueous layer was extracted with ethyl acetate. The combined organic layers were dried over sodium sulfate, filtered, and concentrated to afford the corresponding acid, which was used without purification in the next step.

A mixture of the above acid (410 mg, 1.16 mmol), *O*-tritylhydroxylamine (430 mg, 1.56 mmol), HOBt (237 mg, 1.55 mmol), and EDCI (280 mg, 1.47 mmol) in CH_2Cl_2 was stirred overnight. The reaction mixture was diluted with CH_2Cl_2 and washed with a saturated aqueous solution of NaHCO_3 (3 \times) and water (3 \times) and then dried over sodium sulfate. The solvent was removed, and the crude material was purified by flash chromatography eluting with 0–100% ethyl acetate in hexane to yield the *O*-trityl hydroxamate.

To a solution of the above hydroxamate (50 mg, 0.08 mmol) in CH_2Cl_2 (2 mL) were added triethylsilane (20 mg, 0.17 mmol) and trifluoroacetic acid (88 mg, 0.77 mmol). The reaction mixture was concentrated. The crude material was purified by reverse-phase HPLC (C-18 column) eluting with 5–95% acetonitrile in water to afford **5**. ^1H NMR (400 MHz, CD_3OD): δ 7.43–7.28 (m, 5H, ArH), 7.20–7.16 (m, $J = 8.8$ Hz, 2H, ArH), 6.92–6.88 (m, 2H, ArH), 5.04 (s, 2H, ArCH₂O), 4.12–4.03 (m, 2H, $\text{CO}_2\text{CH}_2\text{CH}_3$), 2.54 (m, 1H, cyclopropyl-CH), 1.98 (dd, 1H, $J = 4.4$ Hz, 6.6 Hz, cyclopropyl-CH), 1.77 (dd, 1H, $J = 4.4$ Hz, 8.8 Hz, cyclopropyl-CH), 1.14 (m, 3 H, $\text{CO}_2\text{CH}_2\text{CH}_3$). LC-MS (ESI) m/z : 356.1 (M + 1) $^+$.

2-(3-Benzyloxyphenyl)-2-trans-carbomethoxycyclopropane Hydroxyamic Acid (4). Compound **4** was prepared following a procedure similar to the synthesis of **5**. ^1H NMR (400 MHz, CD_3CN): δ 7.47–7.33 (m, 5H, ArH), 7.19 (dd, 1H, $J = 7.3$ Hz, 8.8

Hz, ArH), 6.90–6.84 (m, 3H, ArH), 5.08–5.02 (m, 2H, ArCH₂O), 3.56 (s, 3H, CO_2CH_3), 2.49 (dd, 1H, $J = 6.6$ Hz, 8.1 Hz, cyclopropyl-CH), 1.95–1.92 (m, cyclopropyl-CH), 1.72 (dd, 1H, $J = 4.4$ Hz, 8.8 Hz, cyclopropyl-CH). LC-MS (ESI) m/z : 342.1 (M + 1) $^+$.

2-(3-Benzyloxybenzyl)-2-trans-carbomethoxycyclopropane Hydroxyamic Acid (6). ^1H NMR (400 MHz, CD_3CN): δ 7.46–7.31 (m, 5H, ArH), 7.19–7.5 (m, 1H, ArH), 6.87–6.83 (br. s, 1H, ArH), 6.82–6.79 (m, 2H, ArH), 5.07 (s, 2H, OCH_2Ar), 3.56 (s, 3H, CO_2CH_3), 3.19–3.00 (m, 2H, ArCH₂), cyclopropyl-CH), 1.52 (dd, 1H, $J = 3.6$ Hz, 8.8 Hz, cyclopropyl-CH), 1.48–1.45 (m, 1H, cyclopropyl-CH). LC-MS obs: 356.1 (M + 1).

2-(4-Benzyloxybenzyl)-2-trans-carbomethoxycyclopropane Hydroxyamic Acid (7). ^1H NMR (400 MHz, CD_3OD): δ 7.43–7.28 (m, 5H, ArH), 7.15–7.13 (m, 2H, ArH), 6.88–6.86 (m, 2H, ArH), 5.03 (s, 2H, ArCH₂O), 3.60 (s, 3H, CO_2Me), 3.18 (d, $J = 14.6$ Hz, 1H, ArCH₂), 2.97 (d, $J = 14.6$ Hz, 1H, ArCH₂), 2.24 (br s, 1H, cyclopropyl-CH), 1.53–1.51 (m, 2H, cyclopropyl-CH). LC-MS (ESI) m/z : 356.1 (M + 1) $^+$.

Methyl 2-(3-Benzyloxybenzyl) Acrylate (10). Yield, 38%. ^1H NMR (400 MHz, CDCl_3): δ 7.46–7.43 (m, 2H, ArH), 7.41–7.37 (m, 2H, ArH), 7.35–7.31 (m, 1H, ArH), 7.25–7.21 (m, 1H, ArH), 6.87–6.81 (m, 3H, ArH), 6.25 (br s, 1H, vinyl-CH), 5.49–5.48 (m, 1H, vinyl-CH), 5.05 (s, 2H, OCH_2Ar), 3.74 (s, 3H, CO_2CH_3), 3.62 (br s, 2H, CH_2ArO).

Methyl 2-(4-Benzyloxybenzyl) Acrylate (11). A solution of 1.5 M *tert*-butyl lithium in hexane (53 mL, 80 mmol) was added to a solution of **9** (10.5g, 37 mmol) in anhydrous THF (100 mL) at -78 $^\circ\text{C}$ over 5 min. After the solution was stirred at -78 $^\circ\text{C}$ for 1 h, it was added into a mixture of CuCN (3.58 g, 40 mmol) in THF (20 mL) at 0 $^\circ\text{C}$. The solution was stirred for 30 min and then cooled to -78 $^\circ\text{C}$ and added to a solution of methyl 2-(bromomethyl)acrylate (5.2 g, 29 mmol) in THF (20 mL) at -78 $^\circ\text{C}$. The reaction was stirred for 30 min at -78 $^\circ\text{C}$ and then warmed to -10 $^\circ\text{C}$ for 10 min before it was poured into a mixture of saturated NH_4Cl in ice. The mixture was extracted with CH_2Cl_2 , and the residue was chromatographed with 10% EtOAc/hexane to give 6.0 g of the desired product **11** (53%). ^1H NMR (400 MHz, CDCl_3): δ 7.45–7.43 (m, 2H, ArH), 7.41–7.37 (m, 2H, ArH), 7.35–7.31 (m, 1H, ArH), 7.14–7.11 (m, 2H, ArH), 6.93–6.91 (m, 2H, ArH), 6.22 (m, 1H, vinyl-CH) 5.46 (m, 1H, vinyl-CH), 5.05 (s, 2H, OCH_2Ar), 3.74 (s, 3H, CO_2CH_3), 3.58 (s, 2H, CH_2ArO).

tert-Butyl 2-(3-Benzyloxybenzyl)-2-trans-carbomethoxycyclopropane Carboxylate (12). Yield, 270 mg; + 21%. ^1H NMR (400 MHz, CDCl_3): δ 7.45–7.30 (m, 5H, ArH), 7.19–7.15 (m, 1H, ArH), 6.90–6.87 (m, 1H, ArH), 6.85–6.83 (m, 1H, ArH), 6.81–6.78 (m, 1H, ArH), 5.05 (s, 2H, OCH_2Ar), 3.62 (s, 3H, CO_2CH_3), 3.24–3.15 (m, 2H, ArCH₂), 2.46 (dd, 1H, $J = 6.6$ Hz, 8.8 Hz, cyclopropyl-CH), 1.59 (dd, 1H, $J = 4.4$ Hz, 8.8 Hz, cyclopropyl-CH), 1.46 (dd, 1H, $J = 4.4$ Hz, 6.6 Hz, cyclopropyl-CH), 1.37 [s, 9 H, $\text{CO}_2\text{C}(\text{CH}_3)_3$].

tert-Butyl 2-(4-Benzyloxybenzyl)-2-trans-carbomethoxyl Cyclopropane Carboxylate (13). Yield, 39%. ^1H NMR (400 MHz, CDCl_3): δ 7.44–7.41 (m, 2H, ArH), 7.39–7.35 (m, 2H, ArH), 7.33–7.29 (m, 1H, ArH), 7.17–7.13 (m, 2H, ArH), 6.89–6.85 (m, 2H, ArH), 5.03 (s, 2H, OCH_2Ar), 3.63 (s, 3H, CO_2CH_3), 3.13 (s, 2H, ArCH₂), 2.42 (dd, 1H, $J = 6.6$ Hz, 8.8 Hz, cyclopropyl-CH), 1.57 (dd, 1H, $J = 4.4$ Hz, 8.1 Hz, cyclopropyl-CH), 1.46 (dd, 1H, $J = 4.4$ Hz, 6.6 Hz, cyclopropyl-CH), 1.36 [s, 9 H, $\text{CO}_2\text{C}(\text{CH}_3)_3$].

tert-Butyl 2-(3-Benzyloxyphenyl)-2-trans-carbomethoxycyclopropane Carboxylate (20). Compound **20** was prepared by the procedure described for the synthesis of **21** (73%). ^1H NMR (400 MHz, CDCl_3): δ 7.44–7.30 (m, 5H, ArH), 7.24–7.20 (m, 1H, ArH), 6.95–6.88 (m, 3H, ArH), 5.03 (s, 2H, OCH_2Ar), 3.64 (s, 3H, CO_2CH_3), 2.64 (dd, 1H, $J = 6.6$ Hz, 8.8 Hz, cyclopropyl-CH), 1.94 (dd, 1H, $J = 4.4$ Hz, 6.6 Hz, cyclopropyl-CH), 1.80 (dd, 1H, $J = 4.4$ Hz, 8.1 Hz, cyclopropyl-CH), 1.20 [s, 9 H, $\text{CO}_2\text{C}(\text{CH}_3)_3$].

tert-Butyl 2-(3-Hydroxyphenyl)-2-trans-carbomethoxycyclopropane Carboxylate (22). To a solution of **13** (2.0 g, 7 mmol) in 100 mL of methanol was added 10% Pd/C (200 mg). The solution was stirred under H_2 atmosphere until the starting material

disappeared. The solution was filtered, and the solvent was evaporated. The racemic mixture (1.0 g) was resolved with an OD chiral column and eluted with 5% IPA/hexane (120 mL/min). The second enantiomer that eluted at 28.17 min was determined to be the active isomer. ¹H NMR (400 MHz, CDCl₃): δ 7.17–7.14 (m, 1 H, ArH), 6.86–6.84 (m, 1H, ArH), 6.76–6.72 (m, 2H, ArH), 3.65 (s, 3H, CO₂CH₃), 2.63 (dd, 1H, *J* = 6.6 Hz, 8.1 Hz, cyclopropyl-CH), 1.93 (dd, 1H, *J* = 4.4 Hz, 6.6 Hz, cyclopropyl-CH), 1.79 (dd, 1H, *J* = 4.4 Hz, 8.1 Hz, cyclopropyl-CH), 1.20 [s, 9H, CO₂C(CH₃)₃]. ¹H NMR (400 MHz, CDCl₃): δ 7.18–7.14 (m, 1 H, ArH), 6.87–6.85 (m, 1H, ArH), 6.76–6.72 (m, 2H, ArH), 3.65 (s, 3H, CO₂CH₃), 2.63 (dd, 1H, *J* = 6.6 Hz, 8.8 Hz, cyclopropyl-CH), 1.93 (dd, 1H, *J* = 4.4 Hz, 6.6 Hz, cyclopropyl-CH), 1.79 (dd, 1H, *J* = 4.4 Hz, 8.1 Hz, cyclopropyl-CH), 1.20 [s, 9H, CO₂C(CH₃)₃]. The enantiomeric excess for both enantiomers was determined using an analytical OD column to be >99%.

tert-Butyl 2-[3-(2-Methylquinolin-4-yl)methoxyphenyl]-2-trans-carbomethoxycyclopropane Carboxylate (23). 4-Chloromethyl-2-methylquinoline (56 mg, 0.25 mmol), K₂CO₃ (100 mg, 0.72 mmol), tetrabutyl ammonium bromide (20 mg, 0.062 mmol), and the second enantiomer of **22** (48 mg, 0.16 mmol) in CH₂Cl₂ were stirred overnight. The reaction solution was washed with water (3×). The aqueous phase was extracted with CH₂Cl₂ (2×). The organic extracts were combined, dried over sodium sulfate, filtered, and concentrated to afford **23**. ¹H NMR (400 MHz, CD₃OD): δ 8.02 (d, 1H, *J* = 7.3 Hz, quinolinyl-CH), 7.97 (d, 1H, *J* = 8.8 Hz, quinolinyl-CH), 7.74–7.70 (m, 1H, quinolinyl-CH), 7.57–7.53 (m, 1H, quinolinyl-CH), 7.50 (s, 1H, quinolinyl-CH), 7.26–7.22 (m, 1H, ArH), 7.01–6.98 (m, 2H, ArH), 6.93–6.91 (m, 1H, ArH), 5.49 (s, 2H, quinolinyl-CH₂O), 3.62 (s, 3H, CO₂CH₃), 2.68 (s, 3H, quinolinyl-CH₃), 2.60 (dd, 1H, *J* = 6.6 Hz, 8.1 Hz, cyclopropyl-CH), 1.94 (dd, 1H, *J* = 5.1 Hz, 6.6 Hz, cyclopropyl-CH), 1.76 (dd, 1H, *J* = 5.1 Hz, 8.8 Hz, cyclopropyl-CH), 1.14 [s, 9H, COC(CH₃)₃].

2-[3-(2-Methylquinolin-4-yl)methoxyphenyl]-2-trans-carbomethoxycyclopropane Hydroxyamic Acid (26). Compound **26** (30 mg, 0.046 mmol) was prepared from **23** using method similar to compound **7**. ¹H NMR (400 MHz, CD₃OD): δ 8.44 (d, 1H, *J* = 8.1 Hz, quinolinyl-CH), 8.20–8.12 (m, 2H, quinolinyl-CH), 8.07 (s, 1H, quinolinyl-CH), 7.98–7.94 (m, 1H, quinolinyl-CH), 7.30–7.25 (m, 1H, ArH), 7.07–7.04 (m, 2H, ArH), 6.98 (d, 1H, *J* = 8.1 Hz, ArH), 5.91–5.82 (m, 2H, quinolinyl-CH₂O), 3.63 (s, 3H, CO₂CH₃), 3.00 (s, 3H, quinolinyl-CH₃), 2.57 (dd, 1H, *J* = 7.3 Hz, 8.8 Hz, cyclopropyl-CH), 2.01 (dd, 1H, *J* = 4.4 Hz, 6.6 Hz, cyclopropyl-CH), 1.82 (dd, 1H, *J* = 4.4 Hz, 8.8 Hz, cyclopropyl-CH). LC-MS (ESI) *m/z*: 407.1 (M + 1)⁺.

O-Trityl 2-[3-(2-Methylquinolin-4-yl)methoxyphenyl]-2-trans-carboxylcyclopropane Hydroxyamic Acid (27). A solution of 1 N LiOH monohydrate in 1:1 THF:H₂O (2 mL, 2.0 mmol) was added to **25** (30 mg, 0.046 mmol). The reaction was concentrated, and the residue was partitioned between CH₂Cl₂ and a saturated aqueous solution of NH₄Cl. The organic layer was washed with a saturated solution of NH₄Cl (3×) and water (3×) and dried over sodium sulfate. The solvent was removed to afford 25 mg of product (**27**) (86%).

2-[3-(2-Methylquinolin-4-yl)methoxyphenyl]-2-trans-carboxamidocyclopropane Hydroxyamic Acid (29). To a solution of **27** (30 mg, 0.047 mmol) in DMF, ammonium chloride (60 mg, 1.11 mmol), HOBt (60 mg, 0.39 mmol), diisopropylethylamine (0.45 mL, 2.6 mmol), and EDCI (80 mg, 0.42 mmol) were added. The reaction was stirred at room temperature overnight. The reaction mixture was diluted with CH₂Cl₂ and washed with H₂O (3×). The organic layer was dried over sodium sulfate, filtered, and concentrated. The crude material was purified via flash chromatography to afford **28**.

Compound **29** was prepared from **28** following the procedure described for the synthesis of **7**. ¹H NMR (400 MHz, CD₃OD): δ 8.46 (d, 1H, *J* = 8.8 Hz, quinolinyl-CH), 8.21–8.13 (m, 2H, quinolinyl-CH), 8.10 (s, 1H, quinolinyl-CH), 8.00–7.96 (m, 1H, quinolinyl-CH), 7.57 (s, 1H), 7.38–7.34 (m, 1H, ArH), 7.15–7.05 (m, 3H, ArH), 5.95–5.86 (m, 2H, quinolinyl-CH₂O), 3.02 (s, 3H,

quinolinyl-CH₃), 2.56–2.53 (m, 1H, cyclopropyl-CH), 1.90–1.88 (m, 1H, cyclopropyl-CH), 1.72–1.69 (m, 1H, cyclopropyl-CH). LC-MS (ESI) *m/z*: 392.1 (M + 1)⁺.

2-[3-(2-Methylquinolin-4-yl)methoxyphenyl]-2-trans-carbomethoxycyclopropane Hydroxyamic Acid (34). ¹H NMR (400 MHz, CDCl₃): δ 8.43 (d, 1H, *J* = 8.8 Hz, quinolinyl-CH), 8.17–8.11 (m, 3H, quinolinyl-CH), 7.97–7.93 (m, 1H, quinolinyl-CH), 7.25 (d, 2H, *J* = 8.8 Hz, ArH), 7.06 (d, 2H, *J* = 8.8 Hz, ArH), 5.83 (s, 2H, quinolinyl-CH₂O), 3.62 (s, 3H, CO₂CH₃), 3.2–3.3 (m, 2H, ArCH₂), 2.99 (s, 3H, quinolinyl-CH₃), 2.28–2.24 (m, 1H, cyclopropyl-CH), 1.57–1.54 (m, 1H, cyclopropyl-CH). LC-MS (ESI) *m/z*: 421.1 (M + 1)⁺.

(1R,2R)-tert-Butyl 2-Acetoxyphenyl-2-trans-carbomethoxycyclopropane Carboxylate (38). To a solution of **22** (516 mg, 1.8 mmol) in CH₂Cl₂ were added acetic anhydride (0.5 mL, 5.3 mmol) and 4-dimethylaminopyridine (28 mg, 0.23 mmol). After 30 min, the reaction was concentrated. The residue was dissolved in CH₂Cl₂ and washed with 0.1 N HCl (3×), a saturated solution of NaHCO₃ (3×), and H₂O (3×). The organic solution was dried over MgSO₄, filtered, and concentrated to afford **38**. ¹H NMR (400 MHz, CDCl₃): δ 7.32–7.28 (m, 1 H, ArH), 7.16–7.14 (m, 1H, ArH), 7.05–7.03 (m, 2H, ArH), 3.64 (s, 3H, CO₂CH₃), 2.63 (dd, 1H, *J* = 6.6 Hz, 8.8 Hz, cyclopropyl-CH), 2.27 (s, 3H, COCH₃), 1.94 (dd, 1H, *J* = 4.4 Hz, 6.6 Hz, cyclopropyl-CH), 1.81 (dd, 1H, *J* = 4.4 Hz, 8.8 Hz, cyclopropyl-CH), 1.17 [s, 9H, CO₂C(CH₃)₃].

(1R,2R)-2-Acetoxyphenyl-2-trans-carbomethoxycyclopropane Carboxylic Acid (39). A solution of **38** (1.69 g, 5 mmol) in 30% trifluoroacetic acid in CH₂Cl₂ (30 mL) was stirred at room temperature. After 2 h, the reaction was concentrated to yield 1.40 g of **39** (100%). ¹H NMR (400 MHz, CDCl₃): δ 7.34–7.30 (m, 1 H, ArH), 7.16–7.13 (m, 1H, ArH), 7.04–7.01 (m, 2H, ArH), 3.66 (s, 3H, CO₂CH₃), 2.74 (dd, 1H, *J* = 6.6 Hz, 8.8 Hz, cyclopropyl-CH), 2.28 (s, 3H, COCH₃), 1.97 (dd, 1H, *J* = 4.4 Hz, 6.6 Hz, cyclopropyl-CH), 1.94 (dd, 1H, *J* = 4.4 Hz, 8.1 Hz, cyclopropyl-CH).

(1R,2R)-2-Acetoxyphenyl-2-trans-carbomethoxycyclopropane Carboxylic Acid Chloride (40). Oxalyl chloride (4.4 mL, 50 mmol) was added to **39** (1.40 g, 5 mmol) in 7 mL of CH₂Cl₂. A drop of DMF was added, and the reaction was stirred at room temperature. After 3 h, the reaction was concentrated to afford **40**. ¹H NMR (400 MHz, CDCl₃): δ 7.377.33 (m, 1 H, ArH), 7.17–7.15 (m, 1H, ArH), 7.11–7.08 (m, 1H, ArH), 7.07–7.06 (m, 1H, ArH), 3.70 (s, 3H, CO₂CH₃), 3.29 (dd, 1H, *J* = 6.6 Hz, 8.1 Hz, cyclopropyl-CH), 2.29 (s, 3H, COCH₃), 2.12 (dd, 1H, *J* = 5.1 Hz, 6.6 Hz, cyclopropyl-CH), 2.04 (dd, 1H, *J* = 5.1 Hz, 8.1 Hz, cyclopropyl-CH).

Resin Loading of 2-(4-Formyl-3-methoxyphenoxy)ethyl Polystyrene Resin (37). *O*-(2-Trimethylsilylethyl)hydroxyl amine hydrochloride (1.66 g, 9.8 mmol) was added to 2-(4-formyl-3-methoxyphenoxy)ethyl polystyrene resin (1.00 mmol/g, 8.3 g, 8.3 mmol, Novabiochem) suspended in a 10:20:70 solvent mixture of HOAc:CH₃OH:THF. The reaction was agitated at room temperature for 16 days. The resin was washed with DMF, THF, and CH₂Cl₂ sequentially (5×).

A solution of 8 M borane-pyridine complex (15 mL, 120 mmol) was added to the resin (7.55 g) suspended in CH₂Cl₂. The mixture was cooled to 0 °C, and dichloroacetic acid (14 mL, 169 mmol) was added. The reaction was agitated at room temperature. After 7 days, the reaction was quenched with methanol. The resin was washed with acetic acid for 30 min (2×) followed by 2 N NH₃ in MeOH (5×) and DMF (5×). The resin was then rinsed with MeOH, THF, and CH₂Cl₂ sequentially (5×) and dried in vacuo to give **37**.

(1R,2R)-O-Trimethylsilylethyl 2-(3-Acetoxyphenyl)-2-trans-carbomethoxycyclopropane Hydroxyamic Acid on Resin (41). Diisopropylethylamine (2.6 mL, 15 mmol) was added to resin **37** (9.77 g) suspended in 40 mL of CH₂Cl₂. Compound **40** (2.24 g, 7.6 mmol) was added dropwise to the suspension. The reaction was agitated for 3 days. The resin was washed with MeOH, THF, and CH₂Cl₂ sequentially (5×) and dried in vacuo to afford 10.82 g of **41**. A portion of resin **41** (202 mg) was agitated with 50% TFA in CH₂Cl₂ overnight. The filtrate was collected and concen-

trated to afford 22 mg of **42** (51%). The loading level of the final resin was determined to be 0.40 mmol/g. $^1\text{H NMR}$ of **42** (400 MHz, CDCl_3): δ 7.31–7.26 (m, ArH), 7.10–7.09 (d, 1H, $J = 7.3$ Hz, ArH), 6.99–6.98 (m, 2H, ArH), 3.65 (s, 3H, CO_2CH_3), 2.51–2.48 (m, 1H, cyclopropyl-CH), 2.29 (s, 3H, COCH_3), 2.05–2.00 (m, 1H, cyclopropyl-CH), 1.85–1.82 (m, 1H, cyclopropyl-CH). LC-MS (ESI) m/z : 294.1 ($M + 1$) $^+$.

(1R,2R)-O-Trimethylsilylethyl 2-(3-Phenoxy)-2-trans-carbomethoxycyclopropane Hydroxamic Acid on Resin (43). The resin was agitated with 20% piperidine in DMF overnight. The resin was washed with MeOH, THF, and CH_2Cl_2 sequentially ($5\times$) to give resin bound **43**.

(1R,2R)-2-[3-(3,4-Dichlorobenzoyloxy)phenyl]-2-trans-carbomethoxycyclopropane Hydroxamic Acid (44). 1,1'-(Azodicycarbonyl)dipiperidine (43 mg, 0.17 mmol) and 3,4-dichlorobenzyl alcohol (35 mg, 0.20 mmol) were added to **S6.3** (100 mg). The resin was suspended in 3 mL of anhydrous THF under nitrogen, and tributylphosphine (0.06 mL, 0.24 mmol) was added. The final reaction mixture was agitated and heated at 70 $^\circ\text{C}$ overnight. The resin was rinsed with anhydrous THF, and the above procedure was repeated. After 2 days, the resin was washed with MeOH, THF, and CH_2Cl_2 sequentially ($5\times$). The resin was cleaved with 75% TFA in CH_2Cl_2 overnight. The filtrate was concentrated. The crude material was purified via preparative HPLC eluting with 5–95% of acetonitrile in water to give desired product **44**. $^1\text{H NMR}$ (400 MHz, CD_3OD): δ 7.62 (d, 1H, $J = 2.2$ Hz, ArH), 7.53 (d, 1H, $J = 8.1$ Hz, ArH), 7.38 (dd, 1H, $J = 1.5, 8.1$ Hz ArH), 7.21–7.17 (m, 1H, ArH), 6.91–6.87 (m, 3H, ArH), 5.04 (s, 2H, ArCH_2), 3.61 (s, 3H, CO_2CH_3), 2.56 (dd, 1H, $J = 6.6$ Hz, 8.8 Hz, cyclopropyl-CH), 2.00 (dd, 1H, $J = 4.4$ Hz, 6.6 Hz cyclopropyl-CH), 1.78 (dd, 1H, $J = 4.4$ Hz, 8.8 Hz cyclopropyl-CH). LC-MS (ESI) m/z : 410.1 ($M + 1$) $^+$.

(1R,2R)-2-(3-Phenoxyphenyl)-2-trans-carbomethoxycyclopropane Hydroxamic Acid (45). A mixture of resin **43**, 5 μm , 4 \AA molecular sieves (100 mg), copper acetate (10 mg, 0.05 mmol), phenyl boronic acid (24 mg, 0.020 mmol), and diisopropylethylamine (0.05 mL, 0.28 mmol) in 2 mL of CH_2Cl_2 was agitated at rt overnight. The resin was washed with THF ($3\times$) and CH_2Cl_2 ($3\times$). The above procedure was repeated. The resin was washed with 0.1 N EDTA in 2:1 DMF:H $_2\text{O}$ for 30 min ($2\times$) followed by a 1:1 DMF:H $_2\text{O}$ solution with a final wash of MeOH, THF, and CH_2Cl_2 sequentially ($5\times$). The resin was cleaved with 75% TFA in CH_2Cl_2 overnight. After removal of organic solvent, the residue was purified with a C-18 reverse phase column eluting with 5–95% acetonitrile in water to give desired product **45**. $^1\text{H NMR}$ (400 MHz, CD_3OD): δ 7.36–7.32 (m, 2H, ArH), 7.27–7.23 (m, 1H, ArH), 7.11–7.07 (m, 1H, ArH), 7.03–6.99 (m, 3H, ArH), 6.93–6.92 (m, 1H, ArH), 6.87–6.85 (m, 1H, ArH), 3.63 (s, 3H, CO_2CH_3), 2.55 (dd, 1H, $J = 6.6$ Hz, 8.8 Hz cyclopropyl-CH), 2.00 (dd, 1H, $J = 4.4$ Hz, 6.6 Hz cyclopropyl-CH), 1.77 (dd, 1H, $J = 4.4$ Hz, 8.8 Hz cyclopropyl-CH). LC-MS (ESI) m/z : 328.2 ($M + 1$) $^+$.

Loading of Wang Hydroxylamine Resin (46). A solution of acid **24** (0.536 mg, 1.06 mmol), Wang hydroxylamine resin (0.931 g, 1.04 mmol/g), EDCI (0.330 g, 1.72 mmol), NMM (1.10 mL, 10.00 mmol), and HOAt (0.150 g, 1.10 mmol) in CH_2Cl_2 (12 mL) was agitated for 14 h at room temperature. The liquid was drained, and the resin was washed with CH_2Cl_2 ($3\times$), THF ($3\times$), and MeOH ($3\times$) in an alternating sequence. The resin was dried under high vacuum to yield **46** (1.32 g, 0.90 mmol/g).

(1R,2R)-2-trans-Carboxyl-2-[3-(2-methylquinolin-4-yl)methoxyphenyl]cyclopropane Hydroxyamic Acid (47) on Resin. A mixture of resin **46** (1.3 g, 0.90 mmol/g) and 1 M Bu_4NOH in THF (15 mL) was agitated at 60 $^\circ\text{C}$ for 6 h. The liquid was drained, and the resin was washed with 1% AcOH in DMF (2×30 min) followed by an alternating cycle of MeOH ($3\times$), THF ($3\times$), and CH_2Cl_2 ($3\times$). The resulting resin was dried under high vacuum for 4 h.

(1R,2R)-2-trans-Carboisopropoxyl-2-[3-(2-methylquinolin-4-yl)methoxyphenyl]cyclopropane Hydroxyamic Acid (48). EDCI (0.035 g, 0.18 mmol) and DMAP (0.015 g, 0.12 mmol) were added to a mixture of the carboxylic acid resin **47** (0.040 g, 0.9 mmol/g)

in CH_2Cl_2 (2 mL). The resin was agitated for 10 min before the addition of 2-propanol (0.015 mL, 0.20 mmol). This mixture was agitated for 16 h at room temperature. The liquid was drained, and the resin was washed with an alternating cycle of CH_2Cl_2 ($3\times$), THF ($3\times$), and MeOH ($3\times$). The resin was treated with 50% TFA/ CH_2Cl_2 (2 mL) and agitated for 1.5 h. The liquid was drained, and the resin was washed with CH_2Cl_2 ($2\times$). The residue was purified by reverse phase HPLC to provide **48** (0.002 g). LC-MS (ESI) m/z : 372.1 ($M + 1$) $^+$.

(1R,2R)-2-trans-(N-Benzylaminocarbonyl)-2-[3-(2-methylquinolin-4-yl)methoxyphenyl]cyclopropane Hydroxyamic Acid (49). A mixture of the carboxylic acid resin **47** (0.040 g, 0.9 mmol/g), EDCI (0.035 g, 0.18 mmol), HOBt (0.023 g, 0.15 mmol), and NMM (0.020 mL, 0.18 mmol) in NMP (2 mL) was agitated for 20 min before the addition of benzyl amine (0.020 mL, 0.18 mmol). This mixture was agitated for 18 h at room temperature. The liquid was drained, and the resin was washed with an alternating cycle of CH_2Cl_2 ($3\times$), THF ($3\times$), and MeOH ($3\times$). The resin was treated with 50% TFA/ CH_2Cl_2 (2 mL) and agitated for 1 h. The liquid was drained, and the resin was washed with CH_2Cl_2 ($2\times$). Concentration of the liquid afforded compound **49** after purification (21 mg). LC-MS (ESI) m/z : 482.3 ($M + 1$) $^+$.

Acknowledgment. We thank Emily Luk for LC-MS analysis and Dr. T. M. Chan and Rebecca Osterman for help in NMR structural determination.

Supporting Information Available: Table of compounds and LC-MS % purity. This material is available free of charge via the Internet at <http://pubs.acs.org>.

References

- (1) (a) Cerretti, D. P. Characterization of the tumour necrosis factor alpha converting enzyme, TACE/ADAM17. *Biochem. Soc. Trans.* **1999**, *27*, 219–223. (b) Vassalli, P. The pathophysiology of tumor necrosis factors. *Annu. Rev. Immunol.* **1992**, *10*, 411–452.
- (2) (a) Van Assche, G.; Rutgeerts, P. Anti-TNF agents in Crohn's disease. *Exp. Opin. Invest. Drugs* **2000**, *9*, 103–111. (b) Nelson, F. C.; Zask, A. The therapeutic potential of small molecule TACE inhibitors. *Exp. Opin. Invest. Drugs* **1999**, *8*, 383–392. (c) Doggrell, S. A. TACE inhibition a new approach to treating inflammation. *Exp. Opin. Invest. Drugs* **2002**, *11*, 1003–1006.
- (3) Kriegler, M.; Perez, C.; DeFay, K.; Albert, I.; Lu, S. D. A novel form of TNF/cachectin is a cell surface cytotoxic transmembrane protein: ramifications for the complex physiology of TNF. *Cell* **1988**, *53*, 45–53.
- (4) (a) Black, R. A.; Rauch, C. T.; Kozlosky, C. J.; Peschon, J. J.; Slack, J. L.; Wolfson, M. F.; Castner, B. J.; Stocking, K. L.; Reddy, P.; Srinivasan, S.; Nelson, N.; Boiani, N.; Schooley, K. A.; Gerhart, M.; Davis, R.; Fitzner, J. N.; Johnson, R. S.; Paxton, R. J.; March, C. J.; Cerretti, D. P. A metalloproteinase disintegrin that releases tumour-necrosis factor- α from cells. *Nature* **1997**, *385*, 729–733. (b) Moss, M. L.; Jin, S.-L.; Milla, M. E.; Bickett, D. M.; Burkhardt, W.; Carter, H. L.; Chen, W. J.; Clay, W. C.; Didsbury, J. R.; Hassler, D.; Hoffman, C. R.; Kost, T. A.; Lambert, M. H.; Leesnitzer, M. A.; McCauley, P.; McGeehan, G.; Mitchell, J.; Moyer, M.; Pahel, G.; Rocque, W.; Overton, L. K.; Schoenen, F.; Seaton, T.; Su, J. L.; Becherer, J. D. Cloning of a disintegrin metalloproteinase that processes precursor tumour-necrosis factor- α . *Nature* **1997**, *385*, 733–736.
- (5) (a) Newton, R. C.; Solomon, K. A.; Covington, M. B.; Decicco, C. P.; Haley, P. J.; Friedman, S. M.; Vaddi, K. Biology of TACE inhibition. *Ann. Rheum. Dis.* **2001**, *60*, 25–32. (b) Moss, M. L.; White, J. M.; Lambert, M. H.; Andrews, R. C. TACE and other ADAM proteases as targets for drug discovery. *Drug Discovery Today* **2001**, *6*, 417–426.
- (6) (a) Skotnicki, J. S.; Zask, A.; Nelson, F. C.; Albright, J. D.; Levin, J. I. Design and synthetic considerations of matrix metalloproteinase inhibitors. *Ann. N. Y. Acad. Sci.* **1999**, *878*, 61–72. (b) De, B.; Natchus, M. G.; Cheng, M.; Pikul, S.; Almstead, N. G.; Taiwo, Y. O.; Snider, C. E.; Chen, L.; Barnett, B.; Gu, F.; Dowty, M. The next generation of MMP inhibitors: Design and synthesis. *Ann. N. Y. Acad. Sci.* **1999**, *878*, 40–60. (c) Nelson, F. C.; Zask, A. The therapeutic potential of small molecule TACE inhibitors. *Exp. Opin. Invest. Drugs* **1999**, *8*, 383–392.
- (7) Yan, Y.; Shirakabe, K.; Werb, Z. The metalloprotease Kuzbanian (ADAM10) mediates the transactivation of EGF receptor by G protein-coupled receptors. *J. Cell Biol.* **2002**, *158*, 221–226.

- (8) Hattori, M.; Osterfield, M.; Flanagan, J. G. Regulated cleavage of a contact-mediated axon repellent. *Science* **2000**, *289*, 1360–1365.
- (9) Lammich, S.; Kojro, E.; Postina, R.; Gilbert, S.; Pfeiffer, R.; Jasionowski, M.; Haass, C.; Fahrenholz, F. Constitutive and regulated alpha-secretase cleavage of Alzheimer's amyloid precursor protein by a disintegrin metalloprotease. *Proc. Natl. Acad. Sci. U.S.A.* **1999**, *96*, 3922–3927.
- (10) Hartmann, D.; De Strooper, B.; Serneels, L.; Craessaerts, K.; Herreman, A.; Annaert, W.; Umans, L.; Lubke, T.; Lena, I. A.; Von Figura, K.; Saftig, P. The disintegrin/metalloprotease ADAM 10 is essential for Notch signaling but not for alpha-secretase activity in fibroblasts. *Hum. Mol. Genet.* **2002**, *11*, 2615–2624.
- (11) (a) Grootveld, M.; McDermott, M. F. BMS-561392 (Bristol-Myers Squibb). *Curr. Opin. Invest. Drugs* **2003**, *4*, 598–602. (b) Liu, R.; Magolda, R.; Newton, R.; Duan, J.; Vaddi, K.; Madskuie, T.; Qian, M.; Collins, R.; Taylor, T.; Giannaris, J. Pharmacological profile of DPC 333, a selective TACE inhibitor. *Inflammation Res.* **2002**, *51*, A27. (c) Zhang, Y.; Xu, J.; Udata, C.; McDevitt, J.; Cummons, T.; Sun, L.; Zhu, Y.; Li, G.; Rao, V.; Wang, Q.; Gibbons, J. Identification and characterization of Aprarastat (TMI-005), a potent, dual TACE/MMP inhibitor for the treatment of RA. *Ann. Rheum. Dis.* **2005**, *64*, 462–463. (d) Fleischmann, R.; Kivitz, A. J.; Franklin, C.; Pavlik, G. S.; Sridharan, S.; Kirsch, T. M. A randomized, double blind, placebo controlled, sequential dose study of the safety of Apratastat (TMI-005), a novel dual inhibitor of TNF-alpha converting enzyme/metalloproteinase, in patients with rheumatoid arthritis on a background of methotrexate. *Ann. Rheum. Dis.* **2005**, *64*, 132.
- (12) Maskos, K.; Fernandez-Catalan, C.; Humber, R.; Bourenkov, G. P.; Bartunik, H.; Eliestad, G. A.; Reddy, P.; Wolfson, M. F.; Rauch, C. T.; Castner, B. J.; Davis, R.; Clarke, H. R. G.; Petersen, M.; Fitzner, J. N.; Cerretti, D. P.; March, C. J.; Paxton, R. J.; Black, R. A.; Bode, W. Crystal structure of the catalytic domain of human tumor necrosis factor-alpha-converting enzyme. *Proc. Natl. Acad. Sci. U.S.A.* **1998**, *95*, 3408–3412.
- (13) A cyclopropyl dicarboxylate scaffold had been previously explored as potential MMP inhibitors as part of an approach for rigidification of peptide backbones. It was concluded that these scaffolds were "poor mimics of the bound conformation" of the peptidic substrates. Reichelt, A.; Gaul, C.; Frey, R. R.; Kennedy, A.; Martin, S. F. *J. Org. Chem.* **2002**, *67* (12), 4062–4075.
- (14) Majid, T. N.; Knochel, P. A new preparation of highly functionalized aromatic and heteroaromatic zinc and copper organometallics. *Tetrahedron Lett.* **1990**, *31*, 4413–4416.
- (15) Serelis, A. K.; Simpson, G. W. Stereoselectivity in the thermal cycloaddition reactions of tetrafluoroethylene to derivatives of alpha-(4-ethoxyphenyl)acrylic acid. *Tetrahedron Lett.* **1997**, *38*, 4277–4280.
- (16) Von der Saal, W.; Reinhardt, R.; Seidenspinner, H.-M.; Satwitz, J.; Quast, H. Cyclopropanediamines. 3. Pure diastereomers of 1,2-cyclopropanedicarboxylic acids and derivatives. *Liebigs Ann. Chem.* **1989**, 703–712.
- (17) Zhu, Z.; Mazzola, R.; Guo, Z.; Lavey, B.; Sinning, L.; Kozlowski, J.; McKittrick, B.; Shih, N.-Y. Compounds for the treatment of inflammatory disorders. U.S. Patent 6,838,466, 2005.
- (18) For other related linkers, see (a) Stanger, K. J.; Krchnak, V. Polymer-supported N-derivatized, O-linked hydroxylamine for concurrent solid-phase synthesis of diverse N-alkyl and N-H hydroxamates. *J. Comb. Chem.* **2006**, *8* (3), 435–439. (b) Krchnak, V. Solid-phase synthesis of biologically interesting compounds containing hydroxamic acid moiety. *Med. Chem* **2006**, *6* (1), 27–36. (c) Gazal, S.; Masterson, L. R.; Barany, G. Facile solid-phase synthesis of C-terminal peptide aldehydes and hydroxamates from a common backbone amide-linked (BAL) intermediate. *J. Pept. Res.* **2005**, *66* (6), 324–332. (d) Khan, S. I.; Grinstaff, M. W. A facile and convenient solid-phase procedure for synthesizing nucleoside hydroxamic acids. *Tetrahedron Lett.* **1998**, *39* (44), 8031–8034.
- (19) (a) Chan, D. M.; Monaco, K. L.; Wang, R.-P.; Winters, M. New N- and O-arylation with phenylboronic acids and cupric acetate. *Tetrahedron Lett.* **1998**, *39* (19), 2933–2936. (b) Evans, D. A.; Katz, J. L.; West, T. R. Synthesis of diaryl ethers through the copper-promoted arylation of phenols with arylboronic acids. An expedient synthesis of thyroxine. *Tetrahedron Lett.* **1998**, *39* (19), 2937–2940. (c) Combs, A. P.; Saubern, S.; Rafalski, M.; Lam, P. Y. S. Solid supported aryl/heteroaryl C-N cross-coupling reactions. *Tetrahedron Lett.* **1999**, *40* (9), 1623–1626.
- (20) Detailed SAR work for scaffold **30** will be the subject of another paper, and only limited data are listed in Table 2 for discussion.
- (21) (a) Ingram, R. N.; Orth, P.; Strickland, C. L.; Le, H. V.; Madison, V.; Beyer, B. M. Stabilization of the autoproteolysis of TNF-alpha converting enzyme (TACE) results in a novel crystal form suitable for structure-based drug design studies. *Protein Eng., Protein Des. Sel.* **2006**, *19* (4), 155–161. (b) Beyer, B. M.; Ingram, R. N.; Orth, P.; Strickland, C. Crystal structure of human TNF-alpha convertase mutant complexed with inhibitor for use in structure-based rational drug design. U.S. Patent US7138264, 2006.
- (22) Letavic, M. A.; Axt, M. Z.; Barberia, J. T.; Carty, T. J.; Danley, D. E.; Geoghegan, K. F.; Halim, N. S.; Hoth, L. R.; Kamath, A. V.; Laird, E. R.; Lopresti-Morrow, L. L.; McClure, K. F.; Mitchell, P. G.; Natarajan, V.; Noe, M. C.; Pandit, J.; Reeves, L.; Schulte, G. K.; Snow, S. L.; Sweeney, F. J.; Tan, D. H.; Yu, C. H. Synthesis and biological activity of selective pipercolic acid-based TNF-alpha converting enzyme (TACE) inhibitors. *Bioorg. Med. Chem. Lett.* **2002**, *12*, 1387–1390.
- (23) (a) Hirata, T.; Itoh, K.; Misumi, K.; Kuramoto, Y.; Inokuma, K.; Amano, H.; Aoki, S.; Yoshimatsu, T. Discovery of potent, highly selective, and orally active propenohydroxamate TNF-alpha converting enzyme (TACE) inhibitors. *Abstracts of Papers*, 222nd ACS National Meeting, Chicago, IL, Aug 26–30, 2001; American Chemical Society: Washington, DC, 2001; MEDI-262. (b) Hirata, T.; Misumi, K.; Ito, K.; Inokuma, K.; Katayama, K. Preparation of propenohydroxamic acid derivatives as TACE inhibitors for treatment of sepsis, infectious and autoimmune diseases, etc. International patent WO2002018326, 2002. (c) Hirata, A.; Nishimura, H.; Katayama, K.; Tamura, K.; Amano, H.; Sugimoto, K. Preparation of 3-phenyl- and 3-pyridylpropenohydroxamic acid derivatives as new MMP (MMP-3) inhibitors. Japan Patent JP2004277311, 2004.
- (24) Cross, J. B.; Duca, J. S.; Kaminski, J. J.; Madison, V. S. The active site of a zinc-dependent metalloproteinase influences the computed pK(a) of ligands coordinated to the catalytic zinc ion. *J. Am. Chem. Soc.* **2002**, *124*, 11004–11007.
- (25) Navaza, J. AMoRe: An automated package for molecular replacement. *Acta Crystallogr., Sect. A: Found. Crystallogr.* **1994**, *50*, 157–163.
- (26) Bruenger, A. T.; Adams, P. D.; Clore, G. M.; DeLano, W. L.; Gros, P.; Grosse-Kunstleve, R. W.; Jiang, J. S.; Kuszewski, J.; Nilges, M.; Pannu, N. S.; Read, R. J.; Rice, L. M.; Simonson, T.; Warren, G. L. Crystallography & NMR System: A new software suite for macromolecular structure determination. *Acta Crystallogr., Sect. D: Biol. Crystallogr.* **1998**, *54*, 905–921.
- (27) Bruenger, A. T. Free R value: A novel statistical quantity for assessing the accuracy of crystal structures. *Nature* **1992**, *355*, 472–475.

JM0703760